DINAME 2019 - Proceedings of the XVIII International Symposium on Dynamic Problems of Mechanics,
M.A. Savi, T.G. Ritto and W.M. Bessa (Editors), ABCM, Buzios, RJ, Brazil, March 10th to 15th, 2019

An experimental assessment of a reduced order model for a cantilevered flexible cylinder under VIV

Renato Maia Matarazzo Orsino[1], **Wagner Antonio Defensor Filho**[1] **and Celso Pupo Pesce**[1]

[1] Offshore Mechanics Laboratory, Mechanical Engineering Department, Escola Politécnica, University of São Paulo, Av. Professor Lucio Martins Rodrigues, Tv. 4, n. 434, São Paulo - SP, 05508-020, Brazil, reorsino@usp.br, wadfilho@usp.br, ceppesce@usp.br

Abstract: Inspired by the recent applications of the Modular Modeling Methodology for deriving non-linear reduced-order models in Fluid-Structure Interaction problems involving slender cylinders and by an experimental investigation on vortex-induced vibrations (VIV) of a cantilevered flexible cylinders with isotropic and orthotropic bending stiffness and very low mass ratio, this paper aims to provide a preliminary assessment on the adoption of phenomenological models for representing VIV of flexible cylinders. A reduced-order model for a cantilevered flexible cylinder with isotropic bending stiffness under in-line and cross-wise VIV is proposed and corresponding numerical simulations for selected values of reduced velocity are compared to the results obtained in the experiments performed.

Keywords: Fluid-Structure Interaction (FSI), Vortex-Induced Vibrations (VIV), Modular Modeling Methodology, Reduced-Order Modeling (ROM), Experimental Assessment

INTRODUCTION

Recent studies illustrated that the Modular Modeling Methodology (Orsino and Hess-Coelho 2015; Orsino 2016; Orsino 2017) proved to be particularly suitable on the derivation of non-linear FEM (Orsino and Pesce, 2017a; Orsino and Pesce, 2018a) and reduced-order models (Orsino and Pesce, 2018b) for classical problems in Fluid-Structure Interaction of slender flexible pipes conveying fluid. Motivated by technological applications, particularly to riser mechanics, two extensions of these models were proposed in order to start an investigation on the simultaneous effects of internal and external flows on the dynamics of these structures: Orsino, Pesce and Franzini (2017, 2018) focused on the cross-wise VIV effect on a pipe artificially constrained to a planar motion (orthogonal to the external free-stream); Orsino, Pesce and Franzini (2018a), on the other hand, proposed a study of both cross-wise and in-line VIV effects on a flexible pipe with isotropic bending stiffness (which could perform 3D motions). In both studies, VIV effects were modelled phenomenologically, by coupling wake-oscillators to the degrees of freedom adopted for the discretization of structural motions. In the former works, cross-wise VIV was modeled according to a non-linear Var der Pol oscillator proposed by Ogink and Metrikine (2010), whose parameters were originally tuned for VIV of a single-dof rigid cylinder, while in the latter study, the 2-dof extended VIV model introduced by Frazini and Bunzel (2018), in which different Var der Pol oscillators are proposed for in-line and cross-wise wake-oscillations, was adopted.

Even though phenomenological models based on well tuned non-linear Var der Pol oscillators proved to properly model VIV effects on rigid cylinders, an extension of such an approach for VIV of flexible cylinders still requires experimental validation. This paper proposes a preliminary assessment on this topic, by introducing a non-linear reduced-order model for a cantilevered flexible cylinder under VIV, with the same physical properties as the cylinder with isotropic bending stiffness used in the experiments carried out by Defensor Filho (2018) (see also, Defensor Filho, Pesce and Franzini, 2018), which are briefly described in the following section. By selecting representative values of the reduced velocity U^* of the external flow, corresponding to different response branches of the cylinder under VIV, numerical simulations are proposed in an attempt to investigate if the reduced-order model is able to reproduce, both qualitatively and quantively, the responses observed in the experiments.

EXPERIMENTAL INVESTIGATIONS

Motivated by the previous experimental findings described in Fujarra et al. (2001), a further experimental investigation was carried out at NDF-USP Circulating Water Channel (Fig.1) concerning the influence of the frequency ratio parameter, $f_1^* = f_{1x}/f_{1y}$, on the dynamic behavior of four cantilevered flexible cylinders, under the effects of VIV (Defensor Filho, 2018; Defensor Filho, Pesce and Franzini, 2018).

The flexible cylinders were manufactured by molding a polymeric resin (PlatSil Gel-00) over thin aluminum stiffeners (5052 H34 aluminum alloy) with distinct nominal frequency-ratio parameters, $f_1^* = 1,2,3,4$, provided by the stiffeners cross section aspect ratio. The present work focuses on the experiments performed with the isotropic bending stiffness flexible cylinder only (diameter $D = 10$ mm, free span length $L = 400$ mm and a thin aluminum stiffener of squared rectangular cross section of dimensions 2 mm x 2 mm). The measured frequency ratio parameters between its first and

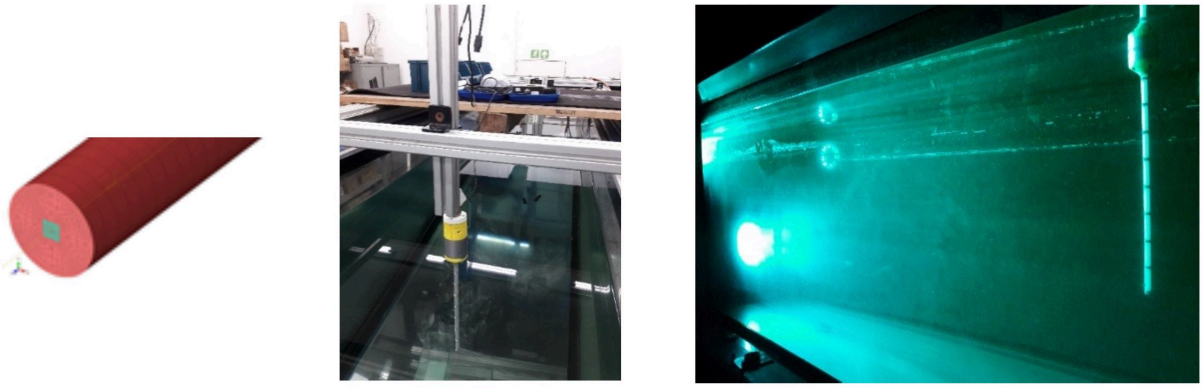

Figure 1: Flexible cylinders with inner squared section stiffener. Experimental mounting. Optical tracking system installed downstream. Extracted from Defensor Filho, Pesce and Franzini (2018).

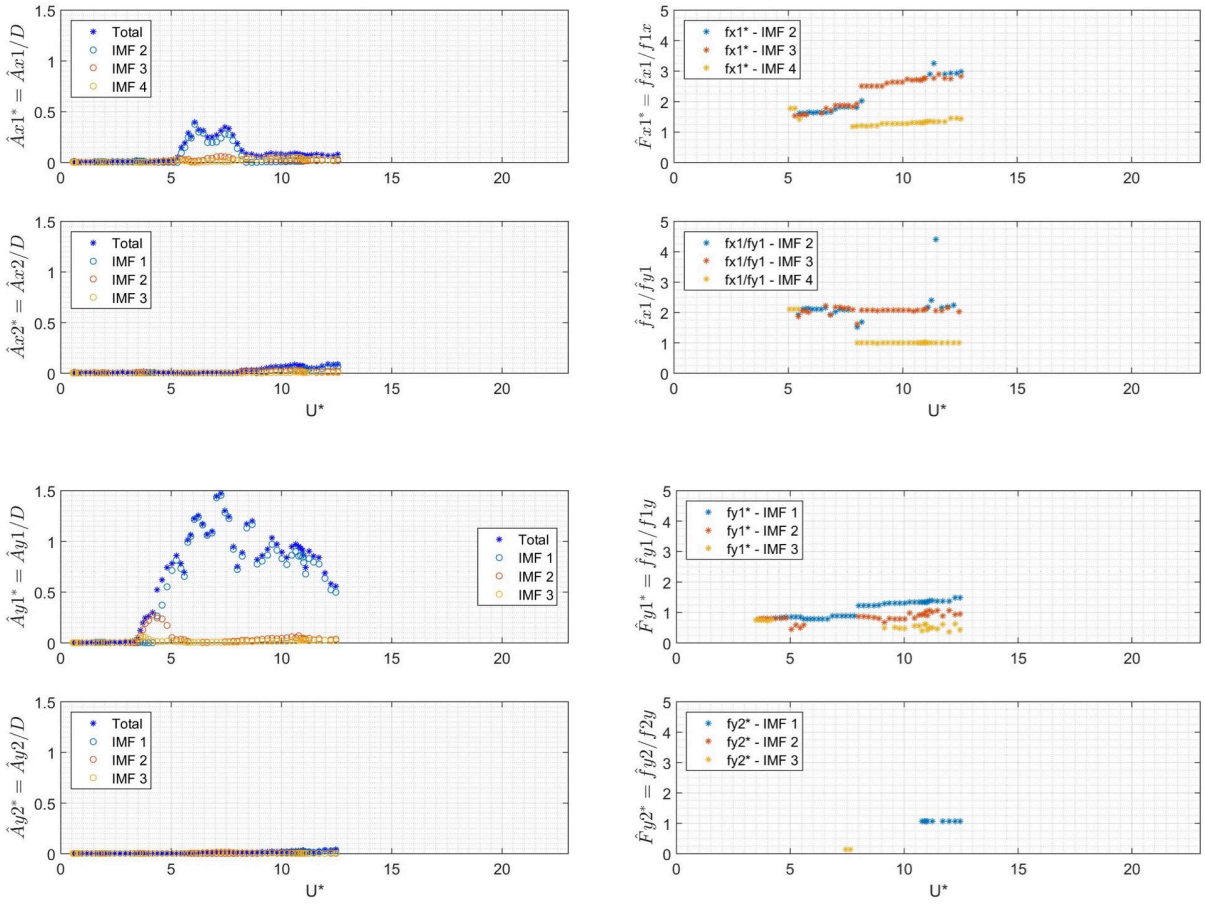

Figure 2: Cantilevered flexible cylinder at nominal natural frequency ratio: modal responses as function of reduced velocities. Left: modal amplitudes - in-line and cross-wise (1st and 2nd modes) and respective IMFs. Right: dominant frequencies ratios. Extracted from Defensor Filho, Pesce and Franzini (2018).

second in-line and crosswise natural frequencies are $f_1^* = f_{1x}/f_{1y} = 1.02$ and $f_2^* = f_{2x}/f_{2y} = 0.97$, respectively.

In that experiment, the maximum reduced-velocity was set to $U^* = 12$, in three repetitive runs. Each run was composed of two parts: an ascending ($U^* = 0$ to 12) and a descending flow speed ($U^* = 12$ to 0) regime; each flow speed regime was divided into twelve values of reduced-velocity, in which the experimental model remained oscillating for at least one hundred oscillations. This procedure, chosen to register the cylinders vibration response during the fluid acceleration/deceleration, led to a very slow and almost linear variation of the flow speed, such that the typical period of vibration is much smaller (circa 1000 less) than the signal acquisition time. A Qualisys underwater optical system was

setted up with 75 Hz sampling frequency and acquired the flexible cylinders vibration continuously by tracking Cartesian coordinates of 9 reflective targets attached along the cylinders span. Reflective tapes, used to line off these targets, were positioned 50 mm apart from each other (center to center distance), except the tapes closest to the clamped and free ends, both positioned 5 mm distant from the extremities. An experimental analysis methodology developed to deal with the vibration response used a combination of techniques such as Galerkin Projection based on Euler-Bernoulli modal shapes, in time domain, Hilbert-Huang Transform (HHT) in a recursive way and a sliding-windowing FFT. To illustrate the results obtained in this analysis, modal amplitudes and dominant frequencies ratios as functions of the reduced velocity U^* are presented in Fig. 2 for first and second modes, for both in-line and cross-wise directions.

REDUCED-ORDER MODEL (ROM)

The reduced-order model proposed for a cantilevered cylinder under VIV is based on the same fundamental hypotheses and follows the same derivation procedure as the one proposed in Orsino, Pesce and Franzini (2018a) for a pipe ejecting fluid under VIV, except from the fact that, in the present model, there is no flow internal to the structure. Denoting by L the Lagrangian of the system (which should contain terms associated to inertial, isotropic flexural stiffness and gravitational effects) and by δW_E the virtual work associated to the interaction with the external flow (lift, drag and added mass effects), the expression of the Extended Hamilton's Principle for this system can be written as follows:

$$\delta \int_{t_1}^{t_2} L\,dt + \int_{t_1}^{t_2} \delta W_\mathrm{E}\,dt = 0 \tag{1}$$

Considering that the experiments were performed in a circulating water channel in which the flow was controlled in order to keep both the magnitude and the horizontal direction of the free-stream velocity constant, a vector basis $(\hat{\mathbf{e}}_\mathrm{x}, \hat{\mathbf{e}}_\mathrm{y}, \hat{\mathbf{e}}_\mathrm{z})$ can be defined so that the unit vector $\hat{\mathbf{e}}_\mathrm{x}$ is aligned with the free-stream velocity $\vec{\mathbf{u}}$ and the unit vector $\hat{\mathbf{e}}_\mathrm{z}$ corresponds to the downward vertical (see Fig. 3). Let ξ be a non-dimensional arc-lenght coordinate defined along the center line of the cylinder and denote by $\vec{\mathbf{r}}$ the non-dimensional position vector of the center of a cross section at a given position ξ with respect to the center of the clamped cross section. Assuming the axial inextensibility of the inner stiffner, $\vec{\mathbf{r}}' = \partial\vec{\mathbf{r}}/\partial\xi = \hat{\mathbf{e}}_\mathrm{t}$ is a unit vector locally tangent to the center line. Therefore, adopting as scales for mass, length and time, respectively, the mass of water displaced by the cylinder m_w of the cylinder, the total lenght l of the cylinder and $\sqrt{m_\mathrm{w} l^3/EI}$, with EI representing the bending stiffness of a cross section, and considering the non-dimensional parameters listed in Table 1, the dimensionless expressions for L and δW_E are the following:

$$L = \frac{1}{2}\int_0^1 \mu\dot{\vec{\mathbf{r}}}\cdot\dot{\vec{\mathbf{r}}} - \frac{1}{2}\int_0^1 \vec{\mathbf{r}}''\cdot\vec{\mathbf{r}}''\,d\xi + \int_0^1 \gamma(\mu-1)\vec{\mathbf{r}}\cdot\hat{\mathbf{e}}_\mathrm{z}\,d\xi \tag{2}$$

$$\delta W_\mathrm{E} = \int_0^1 \left[\frac{2d_\mathrm{e}}{\pi}(\hat{f}_{1y}U^*)^2(C_\mathrm{d}\hat{\mathbf{e}}_\mathrm{d} + C_\ell\hat{\mathbf{e}}_\ell) - \mu_\mathrm{a}\ddot{\vec{\mathbf{r}}}\right]\cdot\delta\vec{\mathbf{r}}\,d\xi \tag{3}$$

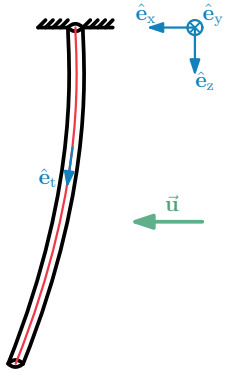

Figure 3: General notation conventions for the proposed model.

Denote by $\vec{\mathbf{u}} = U^*\hat{f}_{1y}d_\mathrm{e}\hat{\mathbf{e}}_\mathrm{x}$ the non-dimensional free-stream velocity and let $\vec{\mathbf{w}} = (\vec{\mathbf{u}} - \dot{\vec{\mathbf{r}}}) - [(\vec{\mathbf{u}} - \dot{\vec{\mathbf{r}}})\cdot\hat{\mathbf{e}}_\mathrm{t}]\,\hat{\mathbf{e}}_\mathrm{t}$ be the projection, in a local cross-section plane, of the non-dimensional relative velocity of the free-stream with respect to the center of the corresponding cross section (see Fig. 4). Based on the 2-dof phenomenological model for VIV proposed by Franzini and Bunzel (2018) originally for a rigid cylinder, the local instantaneous values of the drag (C_d) and lift (C_ℓ) coefficients at a given cross section of the flexible cylinder are computed as follows (see also Table 1):

$$C_\mathrm{d} = \frac{\vec{\mathbf{w}}\cdot\vec{\mathbf{w}}}{u^2}\left[\bar{C}_\mathrm{d}^0 + \frac{q_\mathrm{d}}{\hat{q}}\hat{C}_\mathrm{d}^0\right] \qquad \text{and} \qquad C_\ell = \frac{\vec{\mathbf{w}}\cdot\vec{\mathbf{w}}}{u^2}\frac{q_\ell}{\hat{q}}\hat{C}_\ell^0 \tag{4}$$

Table 1: Non-dimensional parameters of the model and the values adopted in the numerical simulation scenarios adapted from Orsino, Pesce and Franzini (2018a), Franzini and Bunzel (2018) and Defensor Filho (2018).

Parameter	Description	Value
U^*	Reduced velocity	Variable
$\hat{f}_{1y}$	Non-dimensional natural frequency of the first cross-wise bending mode	0.3677
d_e	Non-dimensional external diameter	0.025
γ	Non-dimensional geometric rigidity	0.592
μ	Non-dimensional linear density of the cylinder	1.18
μ_a	Added mass coefficient (Salles and Pesce, 2019)	1.17
$\hat{C}_\ell^0$	Amplitude of the lift coefficient of a stationary cylinder	0.3842
$\bar{C}_\mathrm{d}^0$	Mean drag coefficient of a stationary cylinder	1.1856
$\hat{C}_\mathrm{d}^0$	Amplitude of the drag coefficient of a stationary cylinder	0.2
$\hat{q}$	Limit-cycle amplitude of an unforced Van der Pol oscillator	2
ε_d	Van der Pol parameter of the drag wake-oscillator	$\begin{cases} 0.6, & U^* \leq 8 \\ 0.7, & U^* > 8 \end{cases}$
ε_ℓ	Van der Pol parameter of the lift wake-oscillator	$\begin{cases} 0.0059, & U^* \leq 8 \\ 0.7, & U^* > 8 \end{cases}$
A_d	Acceleration coupling coefficient of the drag wake-oscillator	12
A_ℓ	Acceleration coupling coefficient of the lift wake-oscillator	$\begin{cases} 2, & U^* \leq 8 \\ 12, & U^* > 8 \end{cases}$
St	Strouhal number	0.17

Table 2: Non-dimensional generalized variables of the model.

Variables	Indexes (k)	Description	Definition
r_k	x, y, z	Cartesian coordinates of the center of a cross section	$r_k = \vec{\mathbf{r}} \cdot \hat{\mathbf{e}}_k$
q_k	d, ℓ	In-line and cross-wise wake-oscillator variables	See Eqs. (4) – (6)
$\dot{p}_k$	d, ℓ	Non-linear terms of the Van der Pol oscillators	$\dot{p}_k = (q_k^2 - 1)\dot{q}_k$
$\ddot{a}_k$	d, ℓ	Local in-line and cross-wise components of acceleration	$\ddot{a}_k = \ddot{\vec{\mathbf{r}}} \cdot \hat{\mathbf{e}}_k$
$\dot{c}_k$	x, y, z	Force coefficients associated to x, y, z directions	$\dot{c}_k = (C_\mathrm{d}\hat{\mathbf{e}}_\mathrm{d} + C_\ell\hat{\mathbf{e}}_\ell) \cdot \hat{\mathbf{e}}_k$
$\dot{w}_k$	x, y, z, d	Relative free-stream velocity components	$\dot{w}_k = \vec{\mathbf{w}} \cdot \hat{\mathbf{e}}_k$

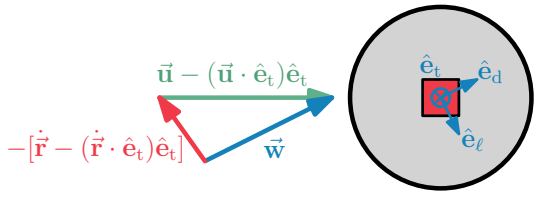

Figure 4: Representation of a cross section of the cylinder, indicating the unit vectors $\hat{\mathbf{e}}_\mathrm{d}$ and $\hat{\mathbf{e}}_\ell$.

with the wake-variables q_d and q_ℓ respecting the following Van der Pol equations, tuned to emulate the phenomenon of dual resonance (notice the double oscillating frequency in the in-line wake oscillator):

$$\ddot{q}_\mathrm{d} + \varepsilon_\mathrm{d}(2\pi\hat{f}_{1y})(StU^*)(q_\mathrm{d}^2 - 1)\dot{q}_\mathrm{d} + (2\pi\hat{f}_{1y})^2(2StU^*)^2 q_\mathrm{d} = \frac{A_\mathrm{d}}{d_\mathrm{e}}\ddot{\vec{\mathbf{r}}} \cdot \hat{\mathbf{e}}_\mathrm{d} \tag{5}$$

$$\ddot{q}_\ell + \varepsilon_\ell(2\pi\hat{f}_{1y})(StU^*)(q_\ell^2 - 1)\dot{q}_\ell + (2\pi\hat{f}_{1y})^2(StU^*)^2 q_\ell = \frac{A_\ell}{d_\mathrm{e}}\ddot{\vec{\mathbf{r}}} \cdot \hat{\mathbf{e}}_\ell \tag{6}$$

As illustrated in Fig. 4, $\hat{\mathbf{e}}_\mathrm{d} = \vec{\mathbf{w}}/w_\mathrm{d}$, with $w_\mathrm{d} = \sqrt{\vec{\mathbf{w}} \cdot \vec{\mathbf{w}}}$, and $\hat{\mathbf{e}}_\ell = \hat{\mathbf{e}}_\mathrm{t} \times \hat{\mathbf{e}}_\mathrm{d}$.

Also following the strategy adopted in Orsino, Pesce and Franzini (2018a) a set of redundant variables is defined, as listed in Table 2, so that, in the derivation of the equations of motion for the model with relaxed constraints, there are no explicit non-linear terms and the discretization procedure can be performed straightforwardly. Let s be any of the variables chosen. Let $\bar{s}(\xi)$ be the value of that variable as if the system could remain at the vertical reference configuration; also,

denote by $\mathbf{h}_s(\xi)$ a column-matrix of projection functions and let $\mathbf{s}(\tau)$ be a column-matrix of generalized variables, so that $s(\tau,\xi)$ can be discretized as follows:

$$s(\tau,\xi) = \bar{s}(\xi) + \mathbf{h}^{\mathsf{T}}(\xi)\mathbf{s}(\tau) \tag{7}$$

Particularly, apart from $\bar{r}_{\mathrm{z}} = \xi$, $\dot{\bar{w}}_{\mathrm{x}} = \dot{\bar{w}}_{\mathrm{d}} = U$ and $\dot{\bar{c}}_{\mathrm{x}} = \bar{C}^0_{\mathrm{d}}$, the reference values of all the other variables defined are identically zero.

Therefore, considering that, according to the Modular Modeling Methodology, both the inextensibility of the stiffner, $\vec{\mathbf{r}}' \cdot \vec{\mathbf{r}}' = 1$, and the conditions relating redundant variables listed in Table 2 can be enforced *a posteriori*, it can be stated that the equations of motion for the model with relaxed constraints can be expressed as follows, for $j = \mathrm{x},\mathrm{y},\mathrm{z}$ and $k = \mathrm{d},\ell$:

$$\begin{cases} (\mu+\mu_{\mathrm{a}})\mathbf{H}_{00}\ddot{\mathbf{r}}_j + \mathbf{H}_{22}\mathbf{r}_j = \dfrac{u^2}{2\pi d_{\mathrm{e}}}\mathbf{H}_{00}\dot{\mathbf{c}}_j + \left[\delta_{j\mathrm{x}}\dfrac{u^2\bar{C}^0_{\mathrm{d}}}{2\pi d_{\mathrm{e}}} + \delta_{j\mathrm{z}}\gamma(\mu-1)\right]\mathbf{h}_0 \\ \ddot{\mathbf{q}}_k + \varepsilon_k(2\pi\hat{f}_{1y})(StU^*)\dot{\mathbf{p}}_k + (2\pi\hat{f}_{1y})^2(\hat{\omega}_k StU^*)^2\mathbf{q}_k = \dfrac{A_k}{\varepsilon}\ddot{\mathbf{a}}_k \end{cases} \tag{8}$$

In these equations, δ_{jk} stands for the Kronecker Delta (i.e., $\delta_{jk} = 1$, if $j = k$ and $\delta_{jk} = 0$, otherwise), $\hat{\omega}_{\mathrm{d}} = 2$ and $\hat{\omega}_{\ell} = 1$. Also:

$$\mathbf{H}_{00} = \int_0^1 \mathbf{h}\mathbf{h}^{\mathsf{T}}\,d\xi, \quad \mathbf{H}_{22} = \int_0^1 \mathbf{h}''\mathbf{h}''^{\mathsf{T}}\,d\xi \quad \text{and} \quad \mathbf{h}_0 = \int_0^1 \mathbf{h}\,d\xi \tag{9}$$

NUMERICAL SIMULATION RESULTS AND COMPARISONS WITH EXPERIMENTAL DATA

Considering the physical properties of the system, as well as observing the results of some experimental tests performed with the manufactured cylinder (Defensor Filho, 2018), it can be stated that the first two modes of structure can be approximated, with a good precision, by the first two modes of a cantilevered Euler-Bernoulli beam, $\phi_1(\xi)$ and $\phi_2(\xi)$. Therefore, the simulations presented in this section correspond to numerical integrations of the equations of motion for the reduced order model obtained by adopting $\mathbf{h}(\xi) = \begin{bmatrix}\phi_1(\xi) & \phi_2(\xi)\end{bmatrix}^{\mathsf{T}}$.

The values of the reduced velocity U^* adopted for comparisons were selected to cover a range of several representative response regimes observed experimentally: $U^* = 4.5$ corresponds to the onset of the cross-wise lock-in region; $U^* = 6$ and $U^* = 7$ correspond to the upper amplitude response branch (upper-branch) of the cross-wise VIV; $U^* = 8$ corresponds to a transition from upper-branch to a subsequent regime (the lower-branch), which had been experimentally inspected by verifying the responses for $U^* = 10$ and $U^* = 12$ (Defensor Filho, Pesce and Franzini, 2018).

The numerical simulation results for the steady-state responses of these scenarios are presented beside the corresponding data measured in the experiments. For selected cross sections, corresponding to some of the centers of the reflective targets attached along the cylinders, the trajectories projected onto the *xy* plane are plotted in Figs. 5 and 6. Once the non-dimensional position coordinates r_{x} and r_{y} adopted in the reduced order model are normalized by the lenght scale of the model, which is the total lenght l of the cylinder and considering that VIV amplitudes are typically normalized by the diameter of the cylinder the x and y coordinates presented in these plots are defined by $x = r_{\mathrm{x}}/d_{\mathrm{e}}$ and $y = r_{\mathrm{y}}/d_{\mathrm{e}}$.

Observing the comparisons presented in Figs. 5 and 6 it can be noticed that apart from the scenario $U^* = 4.5$, the shapes of the curves obtained in the numerical simulations are, at least qualitatively, similar to the ones observed in experiments. The poor agreement observed at $U^* = 4.5$ can be explained by the fact that the phenomenological model adopted imposes an *a priori* dual resonance between in-line and cross-wise VIV, see Eqs. (5) and (6). According to the experimental data, such a phenomenom only takes place in the region $6.0 \leq U^* < 8.0$, in which the best qualitative agreement (among the compared scenarios) was observed in terms of the shape of the trajectories, even though the magnitudes of in-line and cross-wise oscillations were either under or overestimated. For the scenarios $U^* = 10$ and $U^* = 12$, even though a dual resonance response, not so noticiable in the experiments, is present in the simulation results, it can be highlighted the good quantitative agreement in terms of cross-wise oscillation amplitudes (which are not observed in the in-line motion).

FINAL REMARKS

As also discussed in Orsino, Pesce and Franzini (2018a), the derivation of a reduced-order model for a cantilevered flexible cylinder under VIV, based on a modular approach which integrates first-principles and phenomenological models, requires the adoption of some ad-hoc hypotheses which can only be validated experimentally. In this paper, however, it is shown that the adoption of wake-oscillators to represent the effects of in-line and cross-wise VIV of a flexible cylinder is promising. The forced Van der Pol equations coupled to degrees of freedom adopted for the discretization of the motion of the structure were the same ones (regardless even of the mode represented by each degree of freedom) which were originally introduced for describing in-line and cross-wise VIV in a 2-dof rigid cylinder. Even under this *ad-hoc* assumption, a good qualitative agreement on the shape of the trajectories observed in the experiments is achieved, particularly in the range of reduced velocities in which dual resonance phenomenom is more remarkable. These results

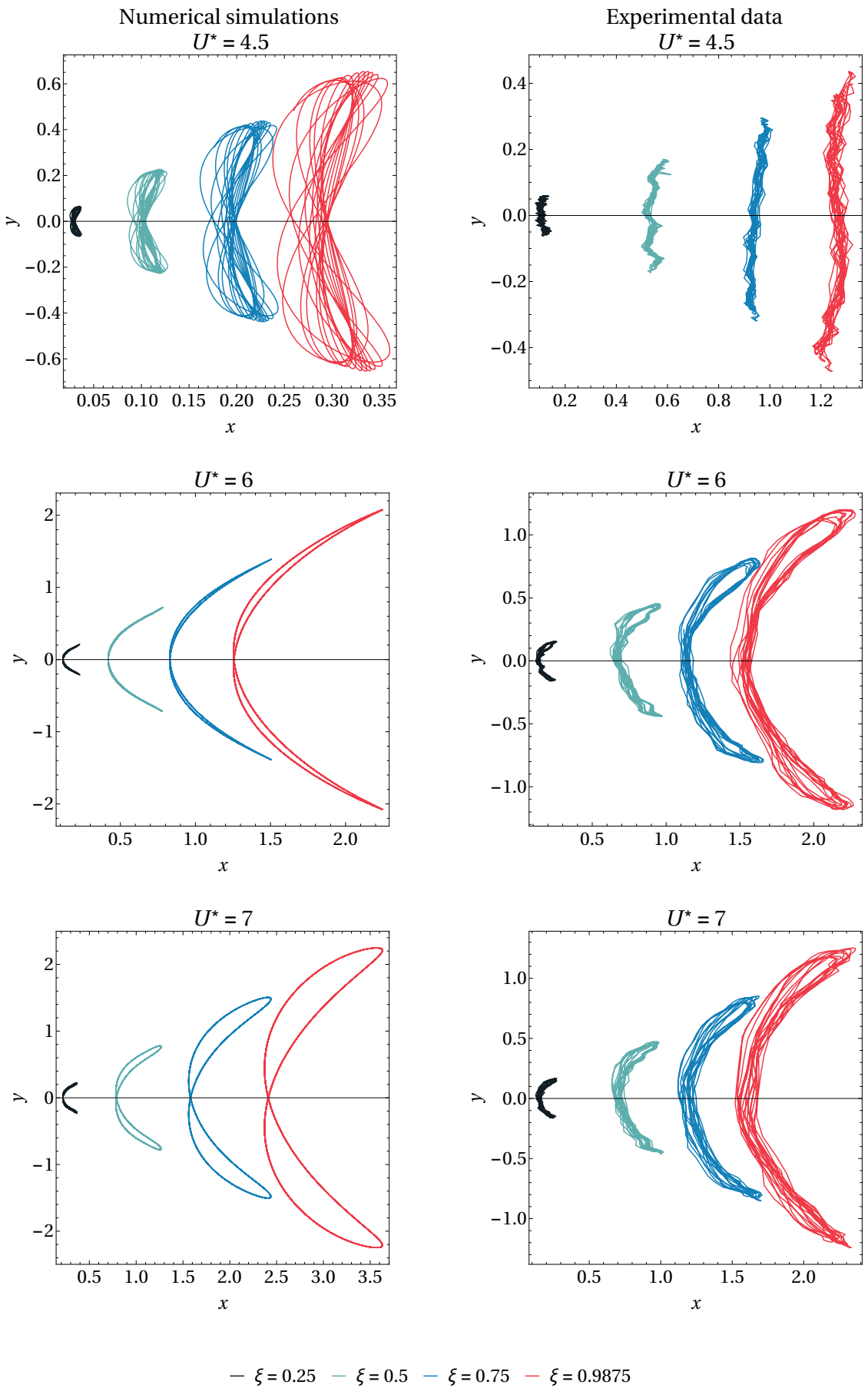

Figure 5: Comparisons between numerical (*left*) and experimental (*right*) steady-state responses: non-dimensional y versus x plots of selected cross-sections for the reduced velocities $U^* = 4.5$, 6 and 7.

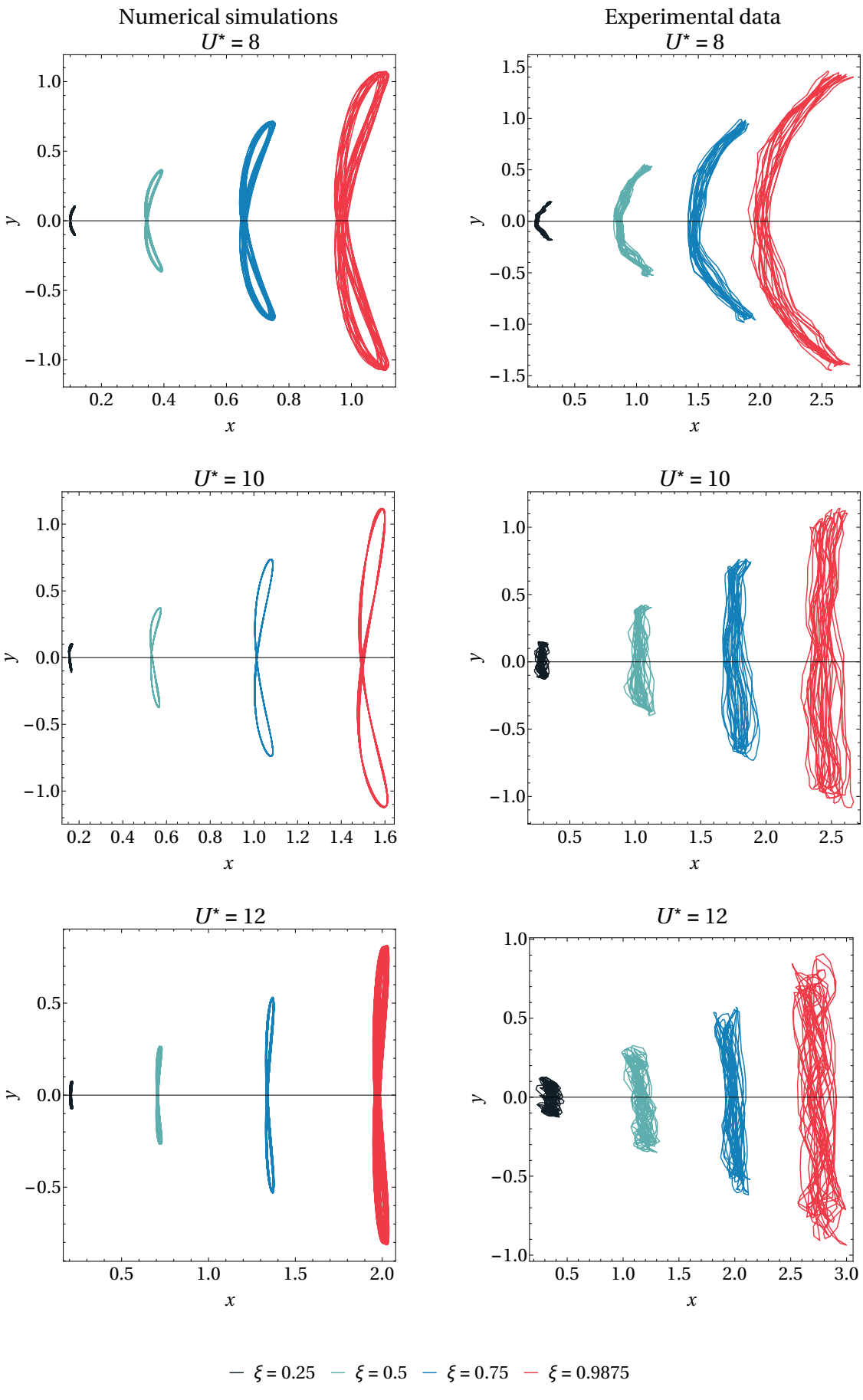

Figure 6: Comparisons between numerical (*left*) and experimental (*right*) steady-state responses: non-dimensional y versus x plots of selected cross-sections for the reduced velocities $U^* = 8$, 10 and 12.

motivate further work on this topic, focusing on adjusting parameters of the wake-oscillator models to fit the response observed in different ranges of reduced velocity for flexible cylinders under VIV, also considering the influence of the particular structural mode to which the oscillator is coupled.

An oncoming work will extend the analyses presented in this paper also for the cases of flexible cantilevered cylinders with orthotropic bending stiffness, which were also object of experimental investigations by Defensor Filho (2018) (see also, Defensor Filho, Pesce and Franzini, 2018), in which other VIV response regimes were observed.

ACKNOWLEDGMENTS

The second author acknowledges a PPGEN Graduate Program in Naval and Ocean Engineering CAPES MSc scholarship; third author acknowledge CNPq research grant n. 308990/2014-5. Authors also thank Dr. Guilherme Rosa Franzini for encouraging discussions.

REFERENCES

Defensor Filho, W. A., 2018, "Investigação experimental de vibrações induzidas por escoamento em cilindros flexíveis com rigidez ortotrópica". MsC Dissertation (in Portuguese), University of São Paulo.

Defensor Filho, W. A.; Pesce, C. P.; Franzini, G. R., 2018, "An experimental investigation on vortex-induced vibrations of cantilevered flexible cylinders with orthotropic bending stiffness". In: *Proceedings of the 9th International Symposium on Fluid-Structure Interactions, Flow-Sound Interactions, Flow-Induced Vibration & Noise*. Toronto, Ontario, Canada. p. 1–9.

Franzini, G. R.; Bunzel, L. O., 2018, "A numerical investigation on piezoelectric energy harvesting from Vortex-Induced Vibrations with one and two degrees of freedom". *Journal of Fluids and Structures*, Elsevier Inc., v. 77, p. 196–212

Fujarra, A. L. C. et al., 2001, "Vortex-induced vibration of a flexible cantilever". *Journal of Fluids and Structures*, v. 15, n. 34, p. 651–658.

Ogink, R. H. M.; Metrikine, A. V., 2010, "A wake oscillator with frequency dependent coupling for the modeling of vortex-induced vibration". *Journal of Sound and Vibration*, Elsevier, v. 329, n. 26, p. 5452–5473.

Orsino, R. M. M., 2016, "A contribution on modeling methodologies for multibody systems". 213 p. PhD thesis, University of São Paulo.

Orsino, R. M. M., 2017, "Recursive modular modelling methodology for lumped-parameter dynamic systems". *Proceedings of the Royal Society A: Mathematical, Physical and Engineering Science*, v. 473, n. 2204.

Orsino, R. M. M.; Hess-Coelho, T. A., 2015, "A contribution on the modular modelling of multibody systems". *Proceedings of the Royal Society A: Mathematical, Physical and Engineering Sciences*, v. 471, n. 2183, p. 1–20.

Orsino, R. M. M.; Pesce, C. P., 2017a, "Novel modular modeling methodology applied to the problem of a pipe conveying fluid". In: *XVII International Symposium on Dynamic Problems of Mechanics, DINAME 2017*. São Sebastião, São Paulo, Brazil.

Orsino, R. M. M.; Pesce, C. P., 2018a, "Modular methodology applied to the nonlinear modeling of a pipe conveying fluid". *Journal of the Brazilian Society of Mechanical Sciences and Engineering*, v. 40, n. 2, p. 67.

Orsino, R. M. M.; Pesce, C. P., 2018b, "Reduced order modeling of a cantilevered pipe conveying fluid applying a modular methodology". *International Journal of Non-Linear Mechanics*, v. 103, p. 1–11.

Orsino, R. M. M.; Pesce, C. P.; Franzini, G. R., 2017, "Cantilevered pipe ejecting fluid under VIV: non-linear reduced order modeling and analysis". In: *24th ABCM International Congress of Mechanical Engineering - COBEM 2017*. Curitiba, Brazil. p. 10.

Orsino, R. M. M.; Pesce, C. P.; Franzini, G. R., 2018a, "A 3D non-linear reduced order model for a cantilevered pipe ejecting fluid under VIV". In: *Proceedings of 9th International Symposium on Fluid-Structure Interactions, Flow-Sound Interactions, Flow-Induced Vibration & Noise, FIV 2018*. Toronto, Canada.

Orsino, R. M. M.; Pesce, C. P.; Franzini, G. R., 2018b, "Cantilevered pipe ejecting fluid under VIV: an investigation based on a planar nonlinear reduced-order model". *Journal of the Brazilian Society of Mechanical Sciences and Engineering*, Springer Berlin Heidelberg, v. 40, n. 11, p. 542.

Salles, R.; Pesce, C. P., 2019, "Experimental Assessments of the Added Mass of Flexible Cylinders in Water: The Role of Modal Shape Representation BT - Proceedings of DINAME 2017". In: Fleury, A. d. T.; Rade, D. A.; Kurka, P. R. G. (Ed.). Springer International Publishing, 2019. p. 215–235.

RESPONSIBILITY NOTICE

The author(s) is (are) the only responsible for the printed material included in this paper.